XLI CILAMCE
XLI Ibero-Latin American Congress on Computational Methods in Engineering
16-19 November, 2020 FOZ DO IGUAÇU PARANÁ - BRAZIL

NUMERICAL ANALYSIS USING DIFFERENT LEVELS OF COMPLEXITY AND DETERMINATION OF ULTIMATE LIMIT STATE FOR RISER CONNECTION DEVICE

Bruno C. Vieceli[1], Filipe P. Geiger[1], Ignacio Iturrioz[1]

[1]*Dept. of Mechanical Engineering, Federal University of Rio Grande do Sul*
Rua Sarmento Leite, 425, ZIP:90050-170, Porto Alegre, Rio Grande do Sul, Brazil
bruno.vieceli@ufrgs.br, filipe.geiger@ufrgs.br, ignacio@mecanica.ufrgs.br

Abstract. In this work, it is presented two methodologies to analyze the Ultimate Limit State (ULS) of a commonly adopted riser connection device named bell mouth (used to decrease the loads that cause excessive bending in the riser) as well as numerical models of said structure, which are compared to a benchmark model. The assessment of the ULS is performed by a standard applicable to steel structures (but not offshore structures) with two different approaches – a traditional one and a, not commonly used, hybrid methodology. The numerical models employ the Finite Element Method with different levels of complexity considered, including elastoplastic behavior, finite deformations and contact formulations (between the bell mouth and cap). Results show an good agreement between the two different ULS approaches. The numerical models provide acceptable similarity with the benchmark model, given its simplicity and low computational cost. It is concluded that the combination of both ULS and numerical analysis may bring a good first iteration in the bell mouth design process.

Keywords: Bell Mouth, Ultimate Limit State, Finite Element Method, Flexible Riser, Hybrid Approach

1 Introduction

Within the context of the offshore oil industry, the transport of crude oil from the seabed to the Floating Production Storage and Offloading (FPSO) unit or semisubmersible unit is made possible using flexible risers. While on operation, they are susceptible to a wide range of loads which are static or dynamic in nature. Given the right circumstances, the riser may fail due to its radius of curvature being too small and thus the bending loads acting on the riser surpassing its limit of acceptance. In order to mitigate such loads, the oil platforms traditionally employ connection devices named bell mouths, as seen in Fig. 1, in its lower balcony region, along with its other ancillary components.

Since the bell mouth is subjected to the aforementioned forces, its structural assessment is of great interest, because a structural failure of any kind in this system may lead to riser rupture and oil spillage in the environment, as well as considerable financial losses.

Even though much research has been made on risers and the adjacent components of the bell mouth, such as bend stiffeners and I-tubes, little is known about the isolated structural behavior of the bell mouth. He, Vaz and Caire [1] have created an analytical model of a riser-bend stiffener with I-tube, where the bending moments, shear and axial forces of such structures are obtained, but the bell mouth is not assessed nor included. That is because many configurations of the coupling between riser and platform are made without its employment in the design, such as the models analyzed by Yucheng, et al. [2]. Traditionally, only the bend stiffener design is assessed, such are the works of Boet and Out [3] and Tanaka, et al. [4], where the riser curvature along its length is one of the main results presented.

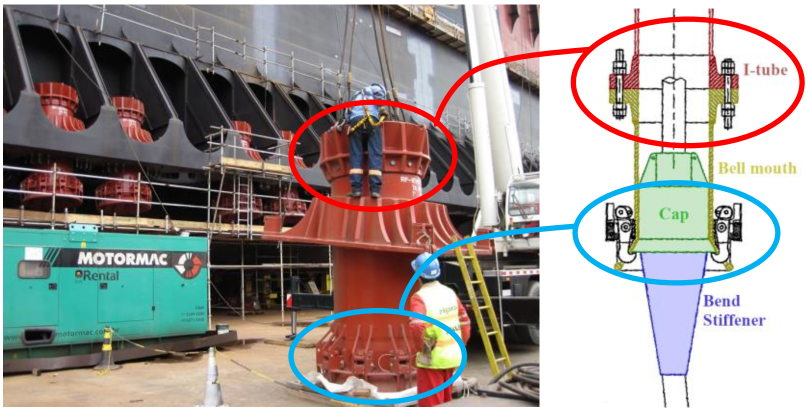

Figure 1. Close up view of FPSO's lower balcony with bell mouths (left) and its adjacent components (right)

A global and local structural analysis of the riser support has been made by Araujo [5] on a semisubmersible platform using the Finite Element Method (FEM), where shear forces and bending moments are applied at reference points on the structure, and the Von Mises stresses are obtained. The fact that the bell mouth is a critical structure in riser design is also reinforced by Rocha, Parrilha and Oliveira [6], where the maximum shear force in a nonlinear dynamic analysis using FEM occurs around the bell mouth location.

To analyze the limit states of metallic structures, particularly the Ultimate Limit State (ULS), Brazilian as well as American standards are commonly used. Perini [7] employed the ABNT NBR 8800 [8] standard in a conventional manner, along with numerical models to address the behavior and ULS of a general structural support. In addition, Ficanha, Nardi and Pravia [9] adopted a hybrid approach proposed by the same standard cited above, as to test its procedure and verify that a number of components with various geometries would comply with the applied loads, which resulted in a satisfactory outcome of this alternative approach.

This work mainly aims to aid the design engineer of a bell mouth system with simple and fast techniques, with the intent to achieve results of a limit state for the structure, as well as observe its expected structural behavior and its critical regions.

The specific objectives are as follows:

• Acquire the ULS using the NBR 8800 standard, with two different approaches.

• Make a structural assessment of the bell mouth by employing the FE Method, in order to acquire the distribution of strains and stresses.

This work is divided in five sections, Section 1 being the first introductory part. Section 2 presents the physical problem, along with its simplifications. Section 3 introduces the methodology and numerical modelling. Results and its discussions are reported in Section 4. Lastly, Section 5 displays the overall conclusions.

2 Physical Model Description

In order to obtain the real results in the bell mouth assessment, every structural member must be employed in the analysis. That is, not only the cap, bend stiffener, I-tube and riser, but also the entirety of the riser support system, since it is subjected to significant deformations, as seen by Araujo [5]. Consequently, it introduces unnecessary complexity and give margin for human and numerical errors.

The model is then simplified to only contain two components: the bell mouth itself and a dummy cap, which is a structure similar to the cap, but its geometry is simplified and has been used to simulate de locking mechanism of the bend stiffener [10]. A sketch of the model is seen in Fig. 2(a). The dimensions for the structure are obtained by the drawings of Teixeira, Longo and Sertã [11], for the 18" bell mouth. Moreover, the bell mouth must be constrained at the top to prevent relative movement between bell mouth and I-tube. A shear load F is also applied at a prescribed distance, which simulates the riser influence on the structure.

The bell mouth is made with A36 structural steel, while the dummy cap uses AISI 1045 steel, both of which have its properties seen in Tab. 1. Their Young's Modulus E and Poisson's ratio ν are set to 207 GPa and 0.3, respectively.

Table 1. Material properties of the bell mouth and dummy cap

Material	Yield Strength f_y (MPa)	Ultimate Tensile Strength (MPa) †	Elongation at break †
A36 Steel	250	400	20%
AISI 1045 Steel	505	585	12%
† Minimum Values			

3 Methodology

3.1 NBR 8800 [8] traditional approach

The traditional employment of this standard is only applicable with slender beams with an equal and continuous cross section. That is not the case for the bell mouth and dummy cap structure, which has a more complex geometry. Nonetheless, one can simplify its design to fit the standard, as seen in Fig. 2.

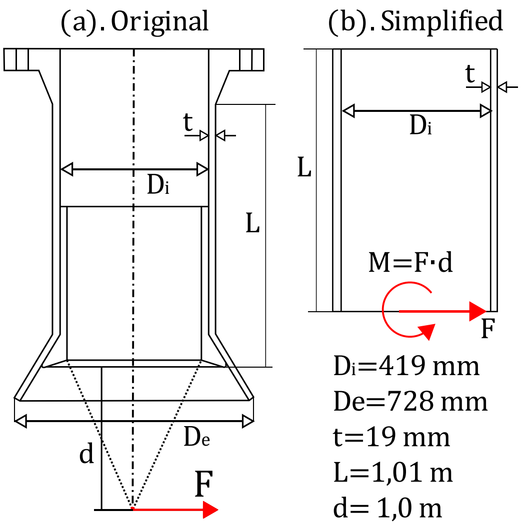

Figure 2. (a) Original bell mouth configuration where the force is applied at a prescribed distance. (b) Simplified geometry created in order to apply the NBR 8800 verification.

The load at which the ULS is reached for the employment of the traditional approach, $\boldsymbol{F_{Sd}^t}$, can be obtained by section 5.4 of the standard, where a limit bending moment and limit shear force are computed. The first of the two to reach the limit state determine the critical load $\boldsymbol{F_{Sd}^t}$.

3.2 NBR 8800 [8] hybrid approach

This general approach does not need simplification on the geometry, so the structure analyzed remains as seen in Fig. 2(a). Section 5.5.2.3 at [8] shows the four possible limit states cases, *I* through *IV*, which are applied here, testing against limit states due to yielding and buckling for normal and shear stresses. To obtain the stress loads $\boldsymbol{\sigma_{Sd,I}}$ and $\boldsymbol{\tau_{Sd,II}}$ seen in eq. (1), a force of unitary value $\boldsymbol{F_1}$ is applied to a linear elastic FEM model. An additional linear buckling analysis is carried out, which also allows for determination of $\boldsymbol{\sigma_{Sd,III}}$ and $\boldsymbol{\tau_{Sd,IV}}$.

$$\sigma_{Sd,I} \leq f_y/\gamma_{a1}, \quad \tau_{Sd,II} \leq 0{,}60 f_y/\gamma_{a1}, \quad \sigma_{Sd,III} \leq \chi f_y/\gamma_{a1} \quad \text{and} \quad \tau_{Sd,IV} \leq 0{,}60\chi f_y/\gamma_{a1}, \tag{1}$$

$\boldsymbol{f_y}$ is the yield strength and $\boldsymbol{\gamma_{a1}}$ is a weighing reduction factor, taken in all cases as unity. The stress distribution acquired from these models is then used to calculate the load at the ULS, F_{Sd}^h, from eq. (2), which is:

$$F_{Sd}^h = \min\{F_{Sd,I}^h, F_{Sd,II}^h, F_{Sd,III}^h, F_{Sd,IV}^h\}. \tag{2}$$

And:

$$F_{Sd,i}^{h} = \alpha_{crit,i} F_1, \;\; i = \{I, II, III, IV\}. \tag{3}$$

Each $\boldsymbol{\alpha_{crit,i}}$ from eq. (3) is a multiplication factor that is obtained by choosing the adequate type of stress for each eq. (1). Equations 4 through 7 shows how to compute each coefficient.

$$\alpha_{crit,I} = f_y/\sigma_{1,m}, \tag{4}$$

$$\alpha_{crit,II} = 1{,}2 f_y/\sigma_{tr,m}, \tag{5}$$

$$\alpha_{crit,III} = \chi f_y/\sigma_{1,m}, \tag{6}$$

$$\alpha_{crit,IV} = 1{,}2 \chi f_y/\sigma_{tr,m}, \tag{7}$$

$\boldsymbol{\sigma_{1,m}}$ and $\boldsymbol{\sigma_{tr,m}}$ are the mean maximum principal stress and mean tresca stress along the thickness of a critical region, respectively, and $\boldsymbol{\chi}$ is a reduction factor associated with buckling or instability. The critical region is defined as having the highest values of stresses associated with each of the four cases of analysis.

To obtain $\boldsymbol{\chi}$, Section 5.3.3 of [8] is used and the critical elastic normal stress $\boldsymbol{\sigma_e}$ and shear stress $\boldsymbol{\tau_e}$ must be computed. This is done with the buckling analysis previously mentioned, and:

$$\sigma_e = \lambda_1 \left|\sigma_{3,mín}\right|, \tag{8}$$

$$\tau_e = \lambda_1 \sigma_{tr,máx}, \tag{9}$$

$\boldsymbol{\lambda_1}$ is the first positive eigenvalue for the associated buckling mode, $\boldsymbol{\sigma_{3,mín}}$ is the minimum value for the minimum principal stress and $\boldsymbol{\sigma_{tr,máx}}$ is the maximum value for the tresca stress.

3.3 Formulation of the FEM Models

The structural assessment of the system is made with the employment of four distinct models, as seen in Tab. 2. Each subsequent model implements more variables to the problem, in order to capture with more precision, the real behavior of the structure.

Table 2. Description of each FEM model

Model	Geometric non-linearity	Contact formulation	Material non-linearity
(a)	Linear	No	Linear Elastic
(b)	Linear	Yes	Linear Elastic
(c)	Non-linear	No	Elastoplastic
(d)	Non-linear	Yes	Elastoplastic

The shear force F from Fig. 2(a) is applied at two different magnitudes. The first, $F^{el} = 100\ kN$, correspond to a state in the linear elastic regime, and thus is applied for cases **(a)** and **(b)**. Another force, which is $F^{pl} = 4F^{el}$, was tested beforehand and deemed sufficient to cause yielding in the structure, hence it will be applied for cases **(c)** and **(d)**.

A benchmark model is also created in the interest of comparison between the simplified models. To make it as similar as possible to the real behavior, this design includes the locking components of the cap, seen in the right side of Fig. 1. Furthermore, it has contact formulations and adequate clearances for all the components, with no geometric simplifications. Physical and geometric non-linearities were likewise employed.

3.4 FEM Modelling

Only half of the geometry is modeled since the force applied is contained in the middle plane of the bell mouth and thus create a symmetry condition. To further simplify the analysis, the gap between the bell mouth and dummy cap, which would exist in the real structure, is removed, in order to facilitate the initial contact for cases **(b)** and **(d)**. Such simplification is deemed sufficiently accurate for the purposes of this work. The contact interaction properties include a friction coefficient of 0.3 (steel to steel, dry) and a normal behavior which forbid penetration of material but allow for separation after contact. A surface to surface contact formulation is employed, where the more refined, external surface of the dummy cap acts as the slave surface, whereas the master surface is the internal bell mouth structure. Also, for cases **(a)** and **(c)**, which do not employ contact formulations, a tie restriction is applied at the nodes of the two bodies where there could be an interaction, in a manner which the assembly behaves as just one body.

The bolts, which connect the top of the bell mouth to the bottom of the I-tube, remove any degrees of freedom and, thus, creating a clamped boundary condition. It is also necessary to create a symmetry condition along the x-y plane. These prescribed displacements are better observed in Fig. 3(a). Figure 3(b) shows the mesh created, where linear hexahedral elements composing of 8 nodes are used in all the analysis.

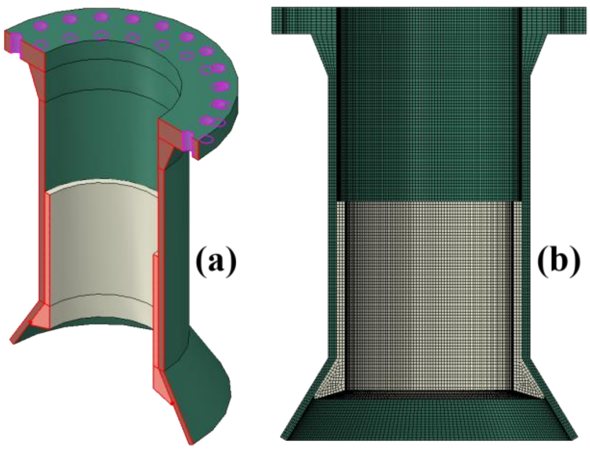

Figure 3. (a) Boundary conditions of symmetry (in red) and clamp (in pink). (b) Mesh employed in the model.

The force is propagated through a Multi-Point Constraint (MPC), which constraints the displacements and rotations of the slave nodes and make it correspond to the state of the reference point. Furthermore, to model the elastoplastic behavior of models **(c)** and **(d)**, the DNV-RP-C208 [12] recommended practice is used, which applies an isotropic hardening rule to both materials and allows for attainment of simplified strain-stress curves.

4 Results

The ULS obtained from both approaches can be seen in Tab. 3. The traditional approach yields a less conservative result of 463 kN, which is somewhat expected due to its employment being for well-established and simple geometries. The hybrid approach, however, provides a result 20% lower, of 388 kN, which accounts for a limit state of buckling due to normal stresses (limit state *III*). This result is almost equal to limit state *I*, which is yielding due to normal stresses. This indicates that plastic deformation of the entire critical region happens somewhat simultaneously with its local buckling.

Also, despite the difference in value of both approaches, they do reach the same order of magnitude. Notice that no additional safety coefficients were considered in these calculations, in order to facilitate the comparison between the different approaches.

Table 3. Forces obtained for ULS for the traditional and hybrid approach

$F_{Sd,I}^{h}$	$F_{Sd,II}^{h}$	$F_{Sd,III}^{h}$	$F_{Sd,IV}^{h}$	F_{Sd}^{h} - Hybrid approach	F_{Sd}^{t} - Traditional approach
391 kN	476 kN	388 kN	474 kN	**388 kN**	**463 kN**

Next, FEM simulations are assessed. It is possible to observe, from Fig. 4, that every model has similar behaviors in its Von Mises stresses distributions, even when comparing between models **(a)** and **(b)** with **(c)** and **(d)**. Cases **(a)** and **(c)**, which do not employ a contact interaction, were not able to reproduce the excessive deformation in the leftmost superior region of contact between the bell mouth and dummy cap, which is a critical detail in its design. Also, yielding has been observed for cases **(c)** and **(d)**, but only the latter could create the expected yielding of the bell mouth in the region cited above.

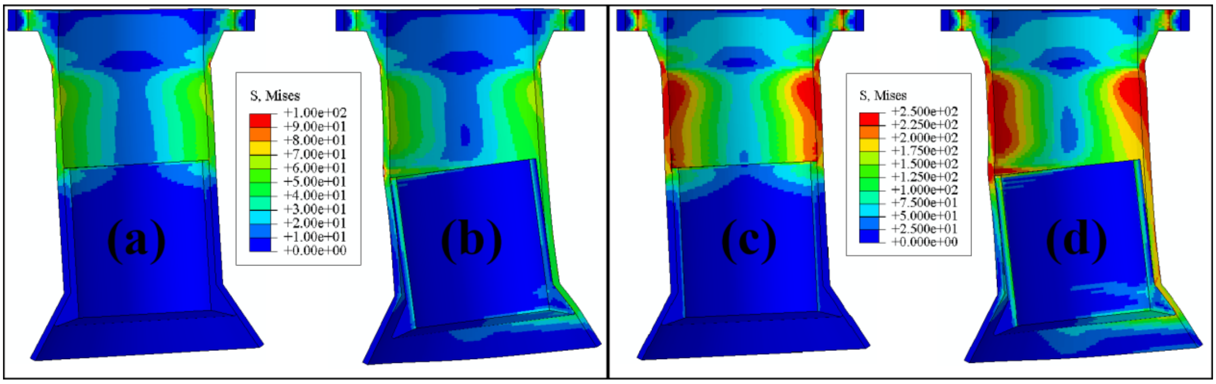

Figure 4. Von Mises stress for the four different FEM models of bell mouth

To check the validity of the linear elastic cases, the strains at the left and right sides of the bell mouth, on its exterior surface and indicated by Fig. 5(a), are compared with the benchmark model. The comparisons can be seen for cases **(a)** and **(b)** on Fig. 5(b).

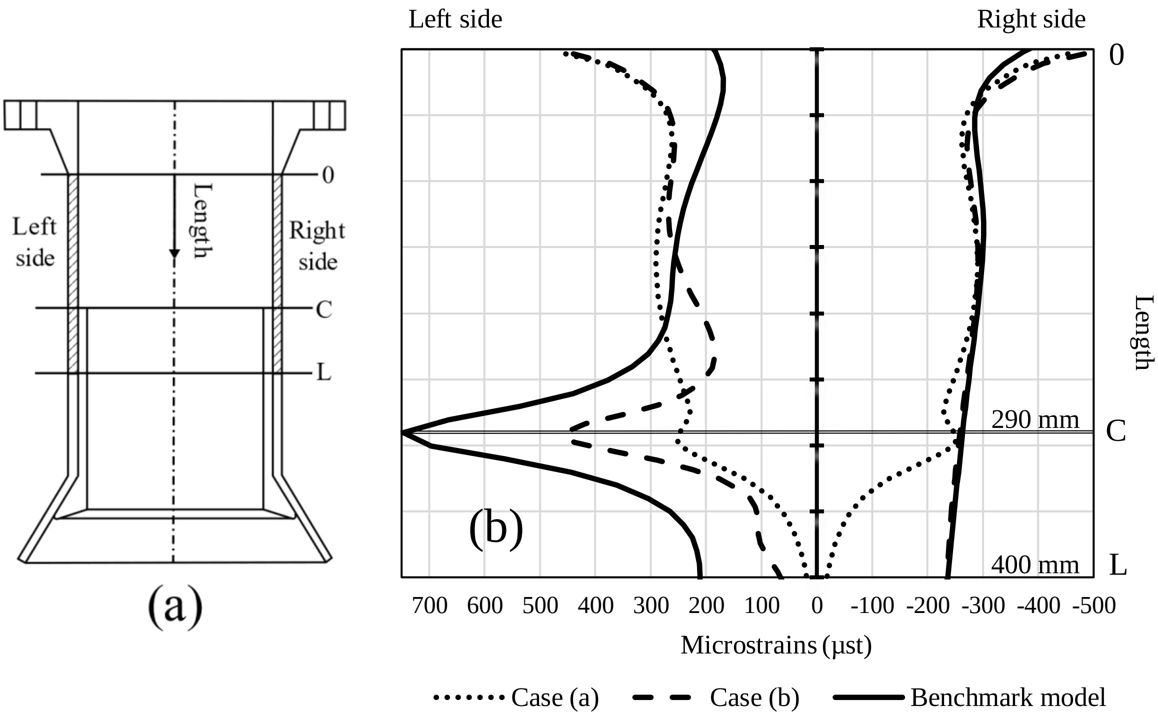

Figure 5. (a) Locations for strains correlations. (b) Comparison of strains with experimental results at the left and right sides of the exterior surface of the bell mouth, for cases where $F = F^{el}$.

While there were differences between the benchmark and the simplified models, one can identify that cases **(a)** and **(b)** provide similar results in order of magnitude and behavior with the benchmark, on regions where the contact of the two bodies plays little to no role. However, for model **(b)**, which exhibits the steep deformations in the contact area at line C, the results were under the expected values, mainly due to a lack of plastic deformation. It could not represent accurately the point of maximum strain, but the same behavior was reached.

Furthermore, the extents of both ULS formulations are approachable through observation of Fig. 4 for cases **(c)** and **(d)**. Yielding in the bell mouth has been observed when $F^{pl} = 400\ kN$ is applied, which is congruent with the limit state load of approximately 390 kN due to yielding/buckling in the hybrid approach. While the traditional approach implied that yielding would only occur when a force $F = 463\ kN$ is applied, the geometry considered was also substantially different from the original, so a discrepancy of behavior between the FEM models and the limit load was likely to happen. Nevertheless, it is of interest to see that both provide results that match the behavior of the numerical models, when regarding the load that causes yielding.

It is important to mention that despite having simplifications applied to the hybrid model, the results presented good agreement to the maximum loading supported by the bell mouth before present yielding. Considering the complexity of the models the methodology here presented shows that as first analysis the hybrid formulations can address the problem with good accuracy and without a high computational cost (when compared to models commonly used).

5 Conclusions

It has been shown that a traditional as well as a hybrid approach to calculate the ULS of a bell mouth structure may potentially be a good procedure to follow in the bell mouth design, since both were able to produce similar results, despite the ABNT NBR 8800 [8] standard not being valid to verify offshore structures. These, aligned with a numerical method of analysis, provide a useful tool to observe the behavior of a bell mouth, with the bonus of little computational time, given the simplicity of the models. While the results for the FEM cases did not reach the benchmark model exactly, especially in the contact region, a safety factor is inherent of the process and aids into the design. Also, the overall behavior of the structure was well established, and one may make design choices based on the critical regions observed.

Authorship statement. The authors hereby confirm that they are the sole liable persons responsible for the authorship of this work, and that all material that has been herein included as part of the present paper is either the property (and authorship) of the authors, or has the permission of the owners to be included here.

References

[1] Y. He, M. A. Vaz and M. Caire, "Flexible riser-bend stiffener top connection analytical model with I-tube," *Marine Structures, vol. 71, p. 102707,* 2020.

[2] H. Yucheng, J. Yuan, Y. Zhang, Z. Tan and T. Sheldrake, "Direct Hang-Off Model to Evaluate Fatigue Damage at Riser Hang-Off," *ASME 2013 32nd International Conference on Ocean, Offshore and Arctic Engineering, vol. 4B, p. 7*, June 2013.

[3] W. Boet e J. Out, "Analysis of a Flexible-Riser Top Connection with Bend Restrictor," *Offshore Technology Conference*, 1990.

[4] R. L. Tanaka, L. M. Y. da Silveira, J. P. Z. Novaes, E. E. de Barros and C. d. A. Martins, "Bending Stiffener Design Through Structural Optimization," *ASME 2009 28th International Conference on Ocean, Offshore and Arctic Engineering, vol. 3*, Maio 2009.

[5] L. G. d. Araujo, "Análise estrutural de suporte de risers," Undergraduate dissertation, *Federal University of Rio de Janeiro*, Rio de Janeiro, 2015.

[6] G. Rocha, R. Parrilha and A. M. Oliveira, "Influence of nonlinear mechanical contact on hang-off location in flexible risers' structural response," *ASME 2010 29th International Conference on Ocean, Offshore and Arctic Engineering, vol. 5, pp. 487-494*, June 2010.

[7] R. Perini, "Comparação de diferentes metodologias de cálculo para determinação da carga de colapso de estruturas metálicas formadas por perfis laminados e soldados," Undergraduate dissertation, *Federal University of Rio Grande do Su*l, Porto Alegre, 2010.

[8] ABNT NBR 8800, "Projeto de estruturas de aço e de estruturas mistas de aço e concreto de edifícios," Rio de Janeiro, 2008.

[9] R. Ficanha, F. A. Nardi and Z. M. C. Pravia, "Dimensionamento de elementos de estruturas de aço usando métodos numéricos," *CONSTRUMETAL 2010 – Congresso Latino-Americano da Construção Metálic*a, August 2010.

[10] CENPES/PDEP/TDUT, "BELL MOUTH SUPPLY SPECIFICATION I-ET-3000.00-1300-279-PPC-203," Rio de Janeiro, 2015.

[11] M. J. B. Teixeira, C. E. V. Longo and S. R. R. Sertã, "Barracuda Field: Installation of 34 Flexible risers in FPSO System," *Offshore Technology Conference*, May 1997.

[12] DNV-RP-C208, "Determination of Structural Capacity by Non-linear FE analysis Methods," 2013.